

Isospin-symmetry breaking in masses of $N \simeq Z$ nuclei

P. Bączyk^a, J. Dobaczewski^{a,b,c,d}, M. Konieczka^a, W. Satuła^{a,d}, T. Nakatsukasa^e, K. Sato^f

^a*Institute of Theoretical Physics, Faculty of Physics, University of Warsaw, ul. Pasteura 5, PL-02-093 Warsaw, Poland*

^b*Department of Physics, University of York, Heslington, York YO10 5DD, United Kingdom*

^c*Department of Physics, P.O. Box 35 (YFL), University of Jyväskylä, FI-40014 Jyväskylä, Finland*

^d*Helsinki Institute of Physics, P.O. Box 64, FI-00014 University of Helsinki, Finland*

^e*Center for Computational Sciences, University of Tsukuba, Tsukuba 305-8577, Japan*

^f*Department of Physics, Osaka City University, Osaka 558-8585, Japan*

Abstract

Effects of the isospin-symmetry breaking (ISB) beyond mean-field Coulomb terms are systematically studied in nuclear masses near the $N = Z$ line. The Coulomb exchange contributions are calculated exactly. We use extended Skyrme energy density functionals (EDFs) with proton-neutron-mixed densities, to which we add new terms breaking the isospin symmetry. Two parameters associated with the new terms are determined by fitting mirror and triplet displacement energies (MDEs and TDEs) of isospin multiplets. The new EDFs reproduce MDEs for the $T = \frac{1}{2}$ doublets and $T = 1$ triplets, and TDEs for the $T = 1$ triplets. Relative strengths of the obtained isospin-symmetry-breaking terms *are not* consistent with the differences in the NN scattering lengths, a_{nn} , a_{pp} , and a_{np} . Based on low-energy experimental data, it seems thus impossible to delineate the strong-force ISB effects from beyond-mean-field Coulomb-energy corrections.

Keywords: nuclear density functional theory (DFT), energy density functional (EDF), proton-neutron mixing, isospin symmetry breaking (ISB), mirror displacement energy (MDE), triplet displacement energy (TDE)

1. Introduction

Similarity between the neutron-neutron (nn), proton-proton (pp), and neutron-proton (np) nuclear forces, commonly known as their charge independence, has been well established experimentally already in 1930's, leading to the concept of the isospin symmetry introduced by Heisenberg [1] and Wigner [2]. Since then, the isospin symmetry has been tested and widely used in theoretical modelling of atomic nuclei, with its explicit violation generated by the Coulomb interaction. In addition, there also exists firm experimental evidence in the nucleon-nucleon (NN) scattering data that the interaction contains small isospin-symmetry-breaking (ISB) components. The differences in the NN phase shifts indicate that the nn interaction, V_{nn} , is about 1% stronger than the pp interaction, V_{pp} , and that the np interaction, V_{np} , is about 2.5% stronger than the average of V_{nn} and V_{pp} [3]. These effects are called charge-symmetry breaking (CSB) and charge-independence breaking (CIB), respectively. In this paper, we show that the manifestation of the CSB and CIB in nuclear masses can systematically be accounted for by the extended nuclear density functional theory (DFT).

The charge dependence of the nuclear strong force fundamentally originates from mass and charge differences between u and d quarks. The strong and electromagnetic interactions among these quarks give rise to the mass splitting among the baryonic and mesonic multiplets. The neutron is slightly heavier than the proton. The pions, which are the Goldstone bosons associated with the chiral symmetry breaking and are the primary carriers of the nuclear force at low energy, also have the mass splitting. The strong-force CSB mostly originates from the difference in masses of protons and neutrons, leading to the difference in the kinetic energies and influencing the one- and two-boson exchange. On the other hand, the major cause of the strong-force CIB is the pion mass splitting. For more details, see Refs. [3, 4].

The Coulomb force is, of course, the major source of ISB in nuclei. In the nuclear DFT, the Coulomb interaction is treated on the mean-field level. Contrary to the atomic DFT, where the exchange and correlation effects are usually treated together [5], in nuclei, the exchange term can be evaluated exactly, as is the case in the present study, but the correlation terms are simply disregarded. Therefore, the ISB terms that we introduce below are meant to describe both the strong-force and Coulomb-correlation effects jointly.

The isospin formalism offers a convenient classification of different components of the nuclear force by dividing them into four distinct classes. Class-I

isoscalar forces are invariant under any rotation in the isospin space. Class-II isotensor forces break the charge independence but are invariant under a rotation by π with respect to the y -axis in the isospace preserving therefore the charge symmetry. Class-III isovector forces break both the charge independence and the charge symmetry, and are symmetric under interchange of two interacting particles. Finally, forces of class IV break both symmetries and are anti-symmetric under the interchange of two particles. This classification was originally proposed by Henley and Miller [4, 6] and subsequently used in the framework of potential models based on boson-exchange formalism, like CD-Bonn [3] or AV18 [7]. The CSB and CIB were also studied in terms of the chiral effective field theory [8, 9]. So far, the Henley-Miller classification has been rather rarely utilized within the nuclear DFT [10, 11], which is usually based on the isoscalar strong forces.

The most prominent manifestation of the ISB is in the mirror displacement energies (MDEs) defined as the differences between binding energies of mirror nuclei:

$$\text{MDE} = BE(T, T_z = -T) - BE(T, T_z = +T). \quad (1)$$

A systematic study by Nolen and Schiffer [12] showed that the MDEs cannot be reproduced by using models involving mean-field Coulomb interaction as the only source of the ISB, see also Refs. [11, 13, 14, 15]. Another source of information on the ISB are the so-called triplet displacement energies (TDEs):

$$\text{TDE} = BE(T=1, T_z = -1) + BE(T=1, T_z = +1) - 2BE(T=1, T_z=0), \quad (2)$$

which are measures of the binding-energy curvatures within the isospin triplets. The TDEs cannot be reproduced by means of conventional approaches disregarding nuclear CIB forces either, see [13, 16]. In the above definitions of MDEs and TDEs, the binding energies are negative ($BE < 0$) and the proton (neutron) has isospin projection of $t_z = -\frac{1}{2}$ ($+\frac{1}{2}$), that is, $T_z = \frac{1}{2}(N - Z)$.

In Fig. 1, we show MDEs and TDEs calculated fully self-consistently using three different standard Skyrme energy-density functionals (EDFs): SV_T [17, 18], SkM* [19], and SLy4 [20]. Details of the calculations, performed using code HFODD [21], are presented in the Supplemental Material [22]. In Fig. 1(a), we clearly see that the values of obtained MDEs are systematically lower than the experimental ones by about 10%. Even more spectacular discrepancy appears in Fig. 1(b) for TDEs, namely, for the $A = 4n$ triplets their

values are nicely reproduced by the mean-field Coulomb effects, however, the characteristic staggering pattern seen in experiment is entirely absent. (See below for the discussion regarding the outlier case of ^{44}V .) It is also very clear that the calculated MDEs and TDEs, which are specific differences of binding energies, are independent of the choice of Skyrme EDF parametrization, that is, of the isoscalar part of the EDF.

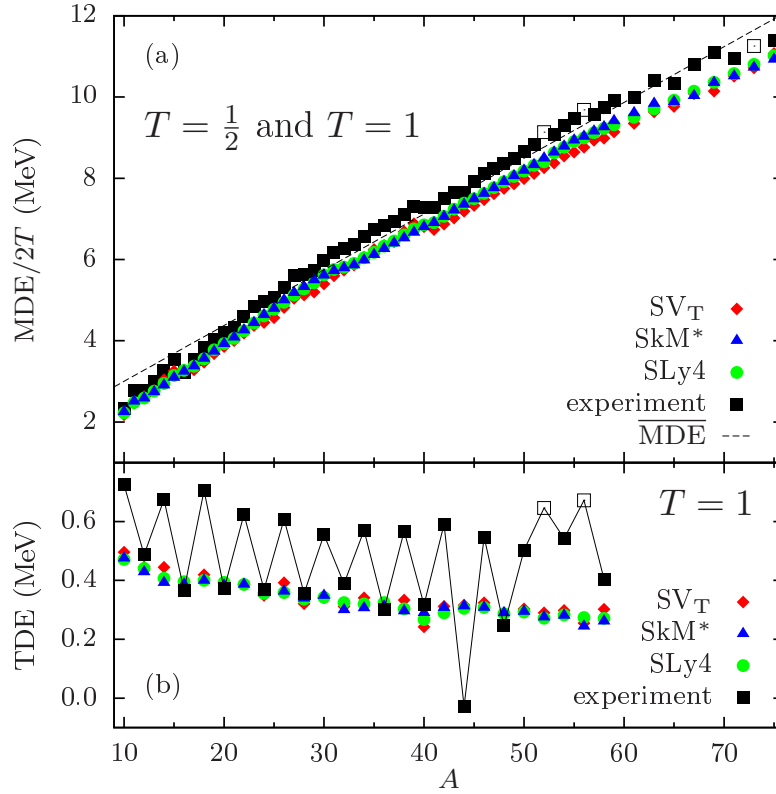


Figure 1: (Color online) Calculated (no ISB terms) and experimental values of MDEs (a) and TDEs (b). The values of MDEs for triplets are divided by two to fit in the plot. Thin dashed line shows the average linear trend of experimental MDEs in doublets, defined as $\overline{MDE} = 0.137A + 1.63$ (in MeV). Measured values of binding energies were taken from Ref. [25] and the excitation energies of the $T = 1$, $T_z = 0$ states from Ref. [26]. Open squares denote data that depend on masses derived from systematics [25].

2. Methods

We aim at a comprehensive study of MDEs and TDEs based on the extended Skyrme pn -mixed DFT [21, 27, 28], which includes zero-range class-II and III forces. We consider the following zero-range interactions of class II and III with two new low-energy coupling constants t_0^{II} and t_0^{III} [29]:

$$\hat{V}^{\text{II}}(i, j) = t_0^{\text{II}} \delta(\mathbf{r}_i - \mathbf{r}_j) \left[3\hat{\tau}_3(i)\hat{\tau}_3(j) - \hat{\tau}(i) \circ \hat{\tau}(j) \right], \quad (3)$$

$$\hat{V}^{\text{III}}(i, j) = t_0^{\text{III}} \delta(\mathbf{r}_i - \mathbf{r}_j) [\hat{\tau}_3(i) + \hat{\tau}_3(j)]. \quad (4)$$

The corresponding contributions to EDF read:

$$\begin{aligned} \mathcal{H}_{\text{II}} = & \frac{1}{2}t_0^{\text{II}}(\rho_n^2 + \rho_p^2 - 2\rho_n\rho_p - 2\rho_{np}\rho_{pn} \\ & - \mathbf{s}_n^2 - \mathbf{s}_p^2 + 2\mathbf{s}_n \cdot \mathbf{s}_p + 2\mathbf{s}_{np} \cdot \mathbf{s}_{pn}), \end{aligned} \quad (5)$$

$$\mathcal{H}_{\text{III}} = \frac{1}{2}t_0^{\text{III}}(\rho_n^2 - \rho_p^2 - \mathbf{s}_n^2 + \mathbf{s}_p^2), \quad (6)$$

where ρ and \mathbf{s} are scalar and spin (vector) densities, respectively. Inclusion of the spin exchange terms in Eqs. (3) and (4) leads to a trivial rescaling of coupling constants t_0^{II} and t_0^{III} , see [29]. Hence, these terms were disregarded.

Contributions of class-III force to EDF (6) depend on the standard nn and pp densities and, therefore, can be taken into account within the conventional pn -separable DFT approach [10, 11]. In contrast, contributions of class-II force (5) depend explicitly on the mixed densities, ρ_{np} and \mathbf{s}_{np} , and require the use of pn -mixed DFT [27, 28].

We implemented the new terms of the EDF in the code HFODD [21], where the isospin degree of freedom is controlled within the isocranking method [27, 30, 31] – an analogue of the cranking technique that is widely used in high-spin physics. The isocranking method allows us to calculate the entire isospin multiplet, T , by starting from an isospin-aligned state $|T, T_z=T\rangle$ and isocranking it around axes tilted with respect to the z -axis. In particular, the isocranking around the x -axis (or equivalently around the y -axis) allows us to reach the state with $\langle \hat{T}_z \rangle \simeq 0$.

A rigorous treatment of the isospin symmetry within the pn -mixed DFT formalism requires full, three-dimensional isospin projection, which is currently under development. However, for the purpose of calculating values of TDEs, we can perform the isospin projection in the following way. First, we

treat the standard effects of the isospin mixing caused by the Coulomb interaction at the mean-field level, cf. [32]. That is, we consider mean-field states of nuclei with $(T, T_z = \pm 1)$ as having approximately good isospin. Then, the only states that need special attention are those with $(T, T_z = 0)$, which are obtained by the isocranking technique.

Let us denote by $|\Psi_{T, T_z}\rangle = \{|\Psi_{1, -1}\rangle, |\Psi_{1, 0}\rangle, |\Psi_{1, 1}\rangle\}$ the wavefunctions of the triplet of states. For the $A = 4n + 2$ triplets, these wave functions can be very simply written as

$$\begin{aligned} |\Psi_{1, -1}\rangle &= a_{p\uparrow}^+ a_{p\downarrow}^+ |0\rangle, \\ |\Psi_{1, 0}\rangle &= \frac{1}{\sqrt{2}} (a_{n\uparrow}^+ a_{p\downarrow}^+ + a_{p\uparrow}^+ a_{n\downarrow}^+) |0\rangle, \\ |\Psi_{1, 1}\rangle &= a_{n\uparrow}^+ a_{n\downarrow}^+ |0\rangle, \end{aligned} \quad (7)$$

where \uparrow and \downarrow denote pairs of Kramers-degenerate deformed states, and $|0\rangle$ denotes the $T = 0$ core of $A = 4n$ particles.

Similarly, the x -isocranked state reads

$$|\Psi_{++}\rangle = a_{+\uparrow}^+ a_{+\downarrow}^+ |0\rangle = \frac{1}{2} |\Psi_{1, -1}\rangle + \frac{1}{\sqrt{2}} |\Psi_{1, 0}\rangle + \frac{1}{2} |\Psi_{1, 1}\rangle, \quad (8)$$

where $|+\uparrow\rangle = \frac{1}{\sqrt{2}} (|n\uparrow\rangle + |p\uparrow\rangle)$ and $|+\downarrow\rangle = \frac{1}{\sqrt{2}} (|n\downarrow\rangle + |p\downarrow\rangle)$ are single-particle eigenstates of the Pauli matrix τ_x . Since all terms in the Hamiltonian are diagonal in T_z , we then have the binding energy of the isocranked state as $BE_{++} = \frac{1}{4} BE(T=1, T_z=-1) + \frac{1}{2} BE(T=1, T_z=0) + \frac{1}{4} BE(T=1, T_z=+1)$. When this result is inserted into Eq. (2), we finally obtain¹

$$\text{TDE} = 2 \left[BE(T=1, T_z=-1) + BE(T=1, T_z=+1) - 2BE_{++} \right]. \quad (9)$$

For the $A = 4n$ triplets, the derivation is slightly more involved, but the same result (9) holds. In this way, TDEs of the isospin-projected triplets can be determined from energies of three Slater determinants: $|\Psi_{1, -1}\rangle$, $|\Psi_{++}\rangle$, and $|\Psi_{1, 1}\rangle$. The procedure proposed in Eqs. (7)–(9) is equivalent to an exact projection on the $N = Z$ $T = 1$ component of the isocranked wavefunction, which amounts to removing its dispersion in T_z .

¹In Refs. [23, 29, 33, 34], we have erroneously used Eq. (2) with $BE(T=1, T_z=0)$ replaced by BE_{++} , which resulted in numerical values of TDEs being twice too small, cf. Eq. (9), and in incorrect values of the adjusted coupling constants t_0^{II} .

Physically relevant values of t_0^{II} and t_0^{III} turn out to be fairly small [29], and thus the new terms do not impair the overall agreement of self-consistent results with the standard experimental data. Moreover, calculated MDEs and TDEs depend on t_0^{II} and t_0^{III} almost linearly, and, in addition, MDEs (TDEs) depend very weakly on t_0^{II} (t_0^{III}) [22, 29]. This allows us to use the standard linear regression method, see, e.g. Refs. [35, 36], to independently adjust t_0^{II} and t_0^{III} to experimental values of TDEs and MDEs, respectively. See Supplemental Material [22] for detailed description of the procedure. Coupling constants t_0^{II} and t_0^{III} resulting from such an adjustment are collected in Table 1. We have performed adjustments to masses tabulated in AME2012 [25]; in this way, below we can test our predictions by comparing the results to those tabulated in AME2016 [37].

Table 1: Coupling constants t_0^{II} and t_0^{III} and their uncertainties obtained in this work for the Skyrme EDFs SV_T^{ISB} , $\text{SkM}^{*\text{ISB}}$, and SLy4^{ISB} . In the last row we show their corresponding ratios.

	SV_T^{ISB}	$\text{SkM}^{*\text{ISB}}$	SLy4^{ISB}
t_0^{II} (MeV fm ³)	4.6 ± 1.6	7 ± 4	6 ± 4
t_0^{III} (MeV fm ³)	-7.4 ± 1.9	-5.6 ± 1.4	-5.6 ± 1.1
$t_0^{\text{II}}/t_0^{\text{III}}$	-0.6 ± 0.3	-1.3 ± 0.8	-1.1 ± 0.7

3. Results

In Fig. 2, we show values of MDEs calculated within our extended DFT formalism for the Skyrme SV_T^{ISB} EDF. By subtracting an overall linear trend (as defined in Fig. 1) we are able to show results in an extended scale, for which a detailed comparison with experimental data is possible. In Fig. 3, we show the corresponding SV_T^{ISB} values of TDEs, whereas complementary results obtained for the Skyrme $\text{SkM}^{*\text{ISB}}$ and SLy4^{ISB} EDFs are collected in the Supplemental Material [22]. Here, we concentrate on the results given by the Skyrme SV_T^{ISB} EDF, because it is the only one based on averaging a two-body pseudopotential (without density-dependent terms), and it is thus free from unwanted self-interaction contributions [38].

It is gratifying to see that the calculated values of MDEs closely follow the experimental A -dependence, see Fig. 2. It is worth noting that a single coupling constant t_0^{III} reproduces both $T = \frac{1}{2}$ and $T = 1$ MDEs, which confirms conclusions of Refs. [10, 11]. In addition, for the $T = \frac{1}{2}$ MDEs,

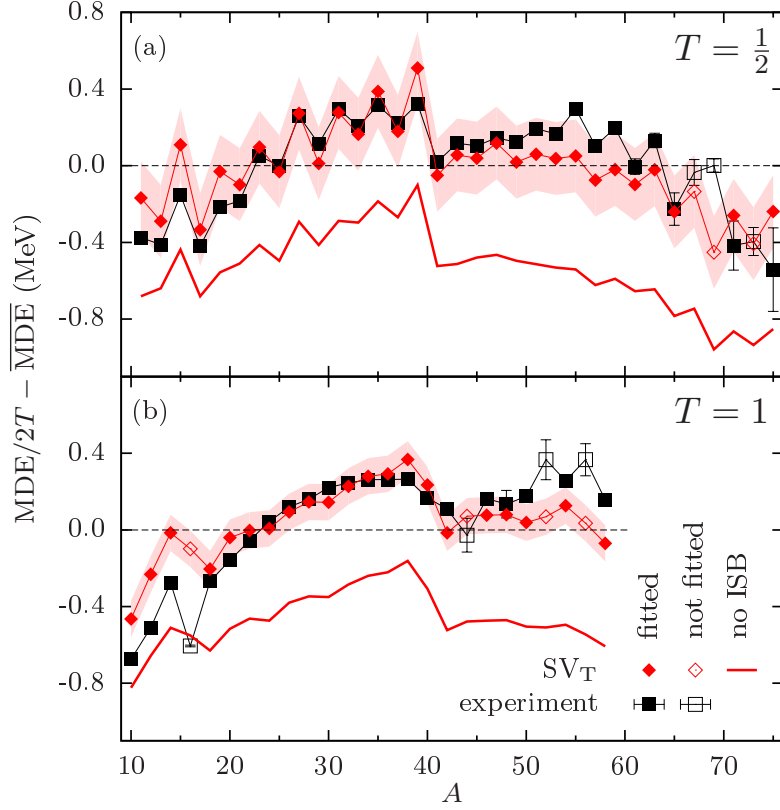


Figure 2: (Color online) Calculated and experimental [25] values of MDEs for the $T = \frac{1}{2}$ (a) and $T = 1$ (b) mirror nuclei, shown with respect to the average linear trend defined in Fig. 1. Calculations were performed for functional SV_T^{ISB} . Shaded bands show theoretical uncertainties. Experimental error bars are shown only when they are larger than the corresponding symbols. Full (open) symbols denote data points included in (excluded from) the fitting procedure.

Fig. 2(a), the SV_T^{ISB} results nicely reproduce (i) changes in experimental trend that occur at $A = 15$ and 39 , (ii) staggering pattern between $A = 15$ and 39 , and (iii) quenching of staggering between $A = 41$ and 53 (the $f_{7/2}$ nuclei).

We note that these features are already present in the SV_T results without the ISB terms, that is, for the mean-field Coulomb interaction. On top of the Coulomb force, the class-III force is essential in bringing the magnitude of MDEs up to the experimental values, but also in simultaneously *increasing* the staggering pattern given by the Coulomb interaction. This is illustrated

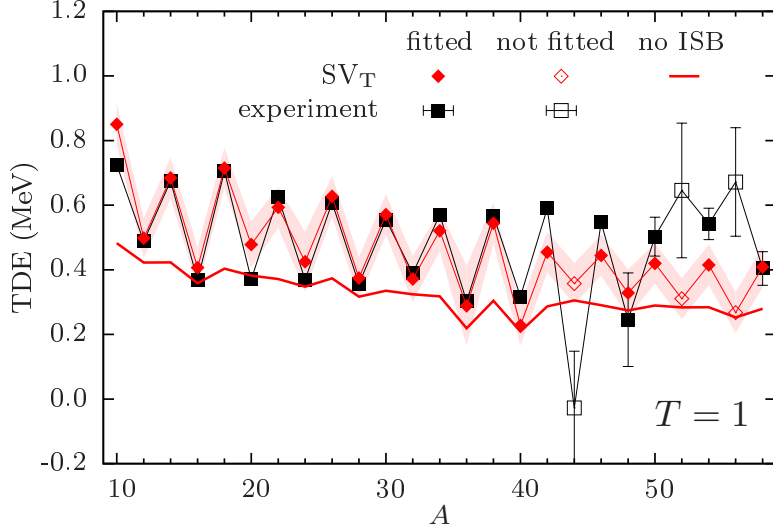


Figure 3: (Color online) Same as in Fig. 2 but for the $T = 1$ TDEs with no linear trend subtracted.

in Fig. 4(a), where we plotted differences $MDE(A) - MDE(A-2)$, separately for the contributions coming from the isoscalar, Coulomb, and class-III terms of the functional.

On the one hand, we see that the Coulomb force alone always induces staggering of MDEs, except in the $f_{7/2}$ and $g_{9/2}$ nuclei, where this part of the staggering disappears almost completely. On the other hand, the class-III force induces a (smaller) *in-phase* staggering in all systems. Because of the self-consistency, the isoscalar terms also show some small out-of-phase staggering, which is a result of strong cancellation between fairly large kinetic-energy and Skyrme-force contributions. In Fig. 4(b), we showed differences $MDE(A) - MDE(A-2)$ calculated with and without the ISB terms, compared with experimental values [25]. This figure also shows results of our calculations extrapolated up to $A = 99$.

For all three functionals our results correctly describe the A -dependence, and lack of staggering, of the $T = 1$ MDEs, see Fig. 2(b) and [22]. Coming to the discussion of TDEs, it is even more gratifying to see in Fig. 3 that our pn -mixed calculations, with one adjusted class-II coupling constant, t_0^{II} , describe absolute values and staggering of TDEs quite well. By including the class-II force into the SV_T parametrization, the overall rms deviations of

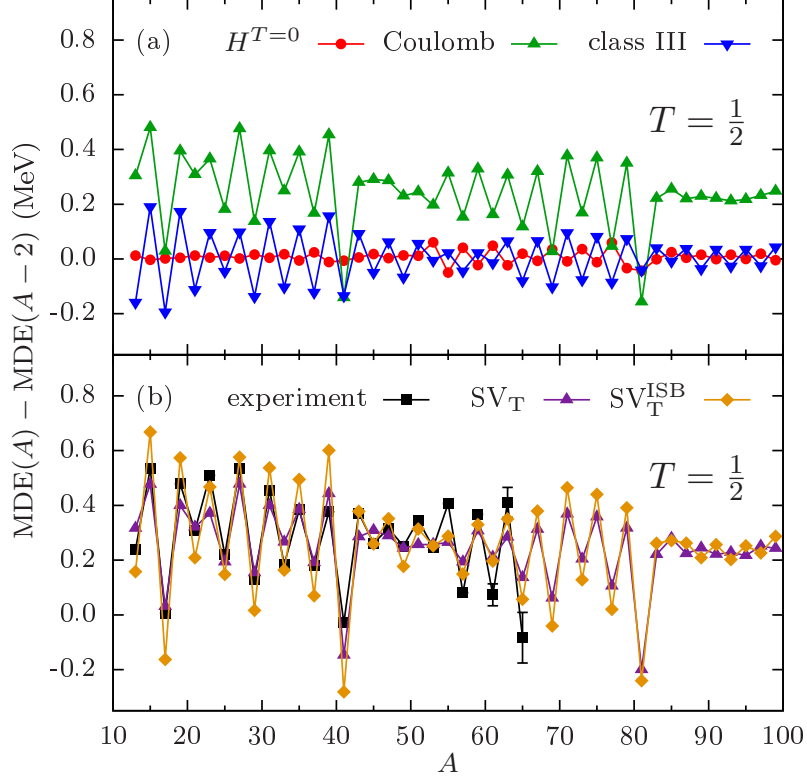


Figure 4: (Color online) Staggering of the calculated $T = \frac{1}{2}$ MDEs: $MDE(A) - MDE(A-2)$. (a) Separate contributions of the isoscalar ($H^{T=0}$), Coulomb, and class-III terms, determined for functional SV_T^{ISB} . (b) Results obtained for functionals SV_T (no ISB) and SV_T^{ISB} (fitted) compared with experimental data [25].

TDEs decreases from 190 to 69 keV. In fact, the improvement comes from the decrease of the rms deviations for the $A = 4n + 2$ triplets, from 250 to 75 keV, whereas those for the $A = 4n$ triplets change very little, from 58 to 60 keV.

We also note that (i) in our approach, the staggering of MDEs in the $f_{7/2}$ shell is increased by the ISB terms, leading to an agreement with data, Fig. 4(b), whereas in the results of Ref. [14] this staggering is decreased by the ISB forces. Also, (ii) in light of our results, the standard interpretation of a phenomenological term in Coulomb energies [12, 39] that is proportional to $(-1)^Z$, is not correct. This term was introduced to remove effects of the

proton Coulomb self-energies. Our calculations treat the Coulomb-exchange terms exactly, and thus are free from self-energies; nevertheless, these exact Coulomb energies do not show any staggering of the TDEs, Fig. 3. Therefore, our results disprove the motivation for introducing a phenomenological $(-1)^Z$ term that generates a uniform staggering of MDEs and TDEs. And (iii) for the SkM*^{ISB} and SLy4^{ISB} functionals, the staggering of the $T = \frac{1}{2}$ MDEs and TDEs is less pronounced than for SV_T^{ISB} [22] and the results obtained without the ISB terms show almost no staggering in $T = \frac{1}{2}$ MDEs. This may suggest that the staggering of Coulomb energies in $T = \frac{1}{2}$ MDEs may be washed out by the self-interaction contributions, which are present in the SkM*^{ISB} and SLy4^{ISB} functionals.

Good agreement obtained for the MDEs and TDEs shows that the role and magnitude of the simplest DFT ISB terms are now firmly established. Nevertheless, some conspicuous deviations of our theoretical predictions with respect to the experiment still remain. This includes (i) overestimated (underestimated) values of MDEs in lighter (heavier) multiplets, (ii) overestimated (underestimated) staggering of MDEs in lighter (heavier) doublets, and (iii) underestimated staggering of TDEs in heavier triplets. This suggests that higher-order DFT ISB terms, that is, gradient terms that would generate dependence on surface properties, may still play some role.

It is very instructive to look at ten outliers that were excluded from the fitting procedure. In Figs. 2 and 3, they are shown by open symbols. They can be classified as (i) five outliers that depend on masses of ⁵²Co, ⁵⁶Cu, and ⁷³Rb, which clearly deviate from the calculated trends for MDEs and TDEs. These masses were not directly measured but were derived from systematics [25]. And (ii) two outliers that depend on the mass of ⁴⁴V, whose ground-state measurement may be contaminated by an unresolved isomer [40, 41, 42]. As well as (iii), large differences between experimental and calculated values are found in MDE for $A = 16, 67$ and 69 . Inclusion of these data in the fitting procedure would significantly increase the uncertainty of adjusted coupling constants. The former two classes of outliers, (i) and (ii), call for improving experimental values, whereas the last one (iii) may be a result of structural effects not included in our model.

Our results can be confronted with the state-of-the-art global analysis performed within the shell-model [13]. There, the MDEs and TDEs were very accurately described by fitting the Coulomb, class-II, and class-III shell-model interactions, separately in five different valence spaces between $A = 10$ and 55 . In addition, values of 14 single-particle energies were also adjusted.

Table 2: Mass excesses of ^{52}Co , ^{56}Cu , ^{73}Rb , and ^{44}V obtained in this work and compared with those of AME2012 [25] and AME2016 [37]. Our predictions were calculated as weighted averages of values obtained from MDEs and TDEs for all three used Skyrme parametrizations. The AME values derived from systematics are labelled with symbol #.

Nucleus	Mass excess (keV)		
	This work	AME2012 [25]	AME2016 [37]
^{52}Co	-34370(40)	-33990(200)#	-34361.0(84)
^{56}Cu	-38650(40)	-38240(200)#	-38643(15)
^{73}Rb	-46100(80)	-46080(100)#	-46080(200)#
^{44}V	-23710(40)	-24120(180)	-24120(180)

As a result of such a 29-parameter fit, the rms deviations between measured and calculated values of MDEs and TDEs were obtained as 44 and 23 keV, respectively. This can be contrasted with our two-parameter fit in SV_T^{ISB} , resulting in the corresponding rms deviations of 220 and 66 keV. (Here, we have used the same set of nuclei as that analyzed in Ref. [13].) Undoubtedly, this shows that by adding higher-order DFT ISB terms, our results can still be improved. Nevertheless, we can conclude that both the DFT and shell-model analyses consistently point to the necessity of using specific ISB terms to account for masses of $N \simeq Z$ nuclei.

Having at hand a model with the ISB interactions included, we can calculate MDEs and TDEs for more massive multiplets, and make predictions of binding energies for neutron-deficient ($T_z = -T$) nuclei. In particular, in Table 2 we present predictions of mass excesses of ^{52}Co , ^{56}Cu , and ^{73}Rb , whose masses were in AME2012 [25] derived from systematics, and ^{44}V , whose ground-state mass measurement is uncertain. Recently, the mass excess of ^{52}Co was measured as $-34361(8)$ [43] or $-34331.6(66)$ keV [44]. These values are in excellent agreement with our prediction, even though the difference between them is still far beyond the estimated (much smaller) experimental uncertainties. We also note that a similar excellent agreement is obtained between our mass excess of ^{56}Cu and that of AME2016 [37]. On the other hand, estimates given in Ref. [42] are outside our error bars.

Assuming that the extracted CSB and CIB effects are, predominantly, due to the ISB in the 1S_0 NN scattering channel, one can attempt relating ratio $t_0^{\text{II}}/t_0^{\text{III}}$ to the experimental scattering lengths. The reasoning follows the work of Suzuki *et al.* [10], who assumed a proportionality between the strengths of CSB and CIB forces and the corresponding scattering lengths [45], that is,

$V_{CSB} \propto \Delta a_{CSB} = a_{pp} - a_{nn}$ and $V_{CIB} \propto \Delta a_{CIB} = \frac{1}{2}(a_{pp} + a_{nn}) - a_{np}$, which, in our case, is equivalent to $t_0^{\text{III}} \propto -\frac{1}{2}\Delta a_{CSB}$ and $t_0^{\text{II}} \propto \frac{1}{3}\Delta a_{CIB}$. Assuming further that the proportionality constants are the same, and taking for the experimental values $\Delta a_{CSB} = 1.5 \pm 0.3$ fm and $\Delta a_{CIB} = 5.7 \pm 0.3$ fm [45], one gets the estimate:

$$\frac{t_0^{\text{II}}}{t_0^{\text{III}}} = -\frac{2}{3} \frac{\Delta a_{CIB}}{\Delta a_{CSB}} = -2.5 \pm 0.5. \quad (10)$$

From the values of coupling constants t_0^{II} and t_0^{III} obtain in this work, we can obtain their ratios as given in Table 1. As we can see, the ratios determined by our analysis of masses of $N \simeq Z$ nuclei with $10 \leq A \leq 75$ have a correct sign but are 2–4 times smaller than the estimate (10) based on properties of the NN forces deduced from the NN scattering experiments.

4. Conclusions

In this Letter, we showed that the nuclear DFT with added two new terms related to the ISB interactions of class II and III is able to systematically reproduce observed MDEs and TDEs of $T = \frac{1}{2}$ and $T = 1$ multiplets. Adjusting only two coupling constants, t_0^{II} and t_0^{III} , we reproduced not only the magnitudes of the MDE and TDE but also their characteristic staggering patterns. The obtained values of t_0^{II} and t_0^{III} turn out to *not agree* with the NN ISB interactions (NN scattering lengths) in the 1S_0 channel. We predicted mass excesses of ^{52}Co , ^{56}Cu , ^{73}Rb , and ^{44}V , and for ^{52}Co and ^{56}Cu we obtained excellent agreement with the recently measured values [37, 43, 44]. To better pin down the ISB effects, accurate mass measurements of the other two nuclei are very much called for.

Our work constitutes the first global DFT study of TDEs in the $T = 1$ isomultiplets. It is based on the introduction of a single class-II ISB term within the pn -mixed DFT [27, 28]. In addition, we confirmed results of Refs. [10, 11], which described the values of MDEs by using a single class-III ISB term. We also showed that the characteristic staggering patterns of MDEs are mostly related to the standard Coulomb effects, whereas those of TDEs require introducing the class-II ISB terms. Altogether, we showed that very simple general DFT ISB terms properly account for all currently available experimental data for MDEs and TDEs.

Finally, we note that our adjusted ISB terms probably jointly include effects of the Coulomb correlations beyond mean field and ISB strong inter-

actions, along with possible many-body ISB correlations induced by them. It does not seem reasonable to expect that low-energy nuclear experimental data would allow for disentangling these distinct sources of the ISB in finite nuclei. In this respect, *ab initio* derivations, such as recently performed for four triplets in Ref. [16], would be very important, provided they cover the entire set of data available experimentally.

Interesting comments by Witek Nazarewicz are gratefully acknowledged. This work was supported in part by the Polish National Science Center under Contract Nos. 2014/15/N/ST2/03454 and 2015/17/N/ST2/04025, by the Academy of Finland and University of Jyväskylä within the FIDIPRO program, by Interdisciplinary Computational Science Program in CCS, University of Tsukuba, and by ImPACT Program of Council for Science, Technology and Innovation (Cabinet Office, Government of Japan). We acknowledge the CIŚ Świerk Computing Center, Poland, and the CSC-IT Center for Science Ltd., Finland, for the allocation of computational resources.

References

- [1] W. Heisenberg, Über den Bau der Atomkerne, *Z. Phys.* 77 (1932) 1.
- [2] E. Wigner, On the consequences of the symmetry of the nuclear hamiltonian on the spectroscopy of nuclei, *Phys. Rev.* 51 (1937) 106–119. doi:10.1103/PhysRev.51.106. URL <http://link.aps.org/doi/10.1103/PhysRev.51.106>
- [3] R. Machleidt, High-precision, charge-dependent Bonn nucleon-nucleon potential, *Phys. Rev. C* 63 (2001) 024001. doi:10.1103/PhysRevC.63.024001. URL <https://link.aps.org/doi/10.1103/PhysRevC.63.024001>
- [4] G. A. Miller, W. H. T. van Oers, *Symmetries and Fundamental Interactions in Nuclei*, World Scientific, 1995.
- [5] R. G. Parr, W. Yang, *Density-Functional Theory of Atoms and Molecules*, Oxford University Press, New York, 1989.
- [6] E. M. Henley, G. A. Miller, *Mesons in Nuclei*, North Holland, 1979.

- [7] R. B. Wiringa, S. Pastore, S. C. Pieper, G. A. Miller, Charge-symmetry breaking forces and isospin mixing in ^8Be , *Phys. Rev. C* 88 (2013) 044333. doi:10.1103/PhysRevC.88.044333.
URL <http://link.aps.org/doi/10.1103/PhysRevC.88.044333>
- [8] M. Walzl, U.-G. Meißner, E. Epelbaum, Charge-dependent nucleon-nucleon potential from chiral effective field theory, *Nuclear Physics A* 693 (3-4) (2001) 663 – 692. doi:[http://dx.doi.org/10.1016/S0375-9474\(01\)00969-1](http://dx.doi.org/10.1016/S0375-9474(01)00969-1).
URL <http://www.sciencedirect.com/science/article/pii/S0375947401009691>
- [9] E. Epelbaum, H.-W. Hammer, U.-G. Meißner, Modern theory of nuclear forces, *Rev. Mod. Phys.* 81 (2009) 1773–1825. doi:10.1103/RevModPhys.81.1773.
URL <https://link.aps.org/doi/10.1103/RevModPhys.81.1773>
- [10] T. Suzuki, H. Sagawa, N. Van Giai, Charge independence and charge symmetry breaking interactions and the Coulomb energy anomaly in isobaric analog states, *Phys. Rev. C* 47 (1993) R1360–R1363. doi:10.1103/PhysRevC.47.R1360.
URL <http://link.aps.org/doi/10.1103/PhysRevC.47.R1360>
- [11] B. A. Brown, W. A. Richter, R. Lindsay, Displacement energies with the Skyrme Hartree-Fock method, *Physics Letters B* 483 (1-3) (2000) 49 – 54. doi:[http://dx.doi.org/10.1016/S0370-2693\(00\)00589-X](http://dx.doi.org/10.1016/S0370-2693(00)00589-X).
URL <http://www.sciencedirect.com/science/article/pii/S037026930000589X>
- [12] J. A. Nolen, Jr, J. P. Schiffer, Coulomb energies, *Ann. Rev. Nucl. Sci.* 19 (1969) 471. doi:10.1146/annurev.ns.19.120169.002351.
URL <http://www.annualreviews.org/doi/abs/10.1146/annurev.ns.19.120169.002351>
- [13] W. Ormand, B. Brown, Empirical isospin-nonconserving Hamiltonians for shell-model calculations, *Nuclear Physics A* 491 (1) (1989) 1 – 23. doi:[http://dx.doi.org/10.1016/0375-9474\(89\)90203-0](http://dx.doi.org/10.1016/0375-9474(89)90203-0).
URL <http://www.sciencedirect.com/science/article/pii/0375947489902030>
- [14] K. Kaneko, Y. Sun, T. Mizusaki, S. Tazaki, Variation in displacement energies due to isospin-nonconserving forces, *Phys. Rev. Lett.* 110 (2013) 172505. doi:10.1103/PhysRevLett.110.172505.
URL <http://link.aps.org/doi/10.1103/PhysRevLett.110.172505>

- [15] G. Colò, H. Sagawa, N. Van Giai, P. F. Bortignon, T. Suzuki, Widths of isobaric analog resonances: A microscopic approach, *Phys. Rev. C* 57 (1998) 3049–3054. doi:10.1103/PhysRevC.57.3049. URL <http://link.aps.org/doi/10.1103/PhysRevC.57.3049>
- [16] W. E. Ormand, B. A. Brown, M. Hjorth-Jensen, Realistic calculations for c coefficients of the isobaric mass multiplet equation in $1p0f$ shell nuclei, *Phys. Rev. C* 96 (2017) 024323. doi:10.1103/PhysRevC.96.024323. URL <https://link.aps.org/doi/10.1103/PhysRevC.96.024323>
- [17] M. Beiner, H. Flocard, N. V. Giai, P. Quentin, Nuclear ground-state properties and self-consistent calculations with the Skyrme interaction: (i). spherical description, *Nuclear Physics A* 238 (1) (1975) 29 – 69. doi:[https://doi.org/10.1016/0375-9474\(75\)90338-3](https://doi.org/10.1016/0375-9474(75)90338-3). URL <http://www.sciencedirect.com/science/article/pii/0375947475903383>
- [18] W. Satuła, J. Dobaczewski, Simple regularization scheme for multireference density functional theories, *Phys. Rev. C* 90 (2014) 054303. doi:10.1103/PhysRevC.90.054303. URL <https://link.aps.org/doi/10.1103/PhysRevC.90.054303>
- [19] J. Bartel, P. Quentin, M. Brack, C. Guet, H.-B. Hkansson, Towards a better parametrisation of Skyrme-like effective forces: A critical study of the SkM force, *Nuclear Physics A* 386 (1) (1982) 79 – 100. doi:[https://doi.org/10.1016/0375-9474\(82\)90403-1](https://doi.org/10.1016/0375-9474(82)90403-1). URL <http://www.sciencedirect.com/science/article/pii/0375947482904031>
- [20] E. Chabanat, P. Bonche, P. Haensel, J. Meyer, R. Schaeffer, A Skyrme parametrization from subnuclear to neutron star densities Part II. Nuclei far from stabilities, *Nuclear Physics A* 635 (1) (1998) 231 – 256. doi:[https://doi.org/10.1016/S0375-9474\(98\)00180-8](https://doi.org/10.1016/S0375-9474(98)00180-8). URL <http://www.sciencedirect.com/science/article/pii/S0375947498001808>
- [21] N. Schunck, J. Dobaczewski, W. Satuła, P. Bączyk, J. Dudek, Y. Gao, M. Konieczka, K. Sato, Y. Shi, X. Wang, T. Werner, Solution of the Skyrme-Hartree-Fock-Bogolyubov equations in the Cartesian deformed harmonic-oscillator basis. (VIII) HFODD (v2.73y): A new version of the program, *Computer Physics Communications* 216 (2017) 145 – 174. doi:<https://doi.org/10.1016/j.cpc.2017.03.007>. URL <http://www.sciencedirect.com/science/article/pii/S0010465517300942>

- [22] See Supplemental Material at [URL will be inserted by publisher], which includes Refs. [23, 24], for details of the calculations performed using code HFODD, description of the fitting procedure, and results obtained for the Skyrme SkM* and SLy4 EDFs.
- [23] P. Bączyk, J. Dobaczewski, M. Konieczka, T. Nakatsukasa, K. Sato, W. Satuła, Mirror and triplet displacement energies within nuclear DFT: Numerical stability, *Acta Phys. Pol. B* 48 (2017) 259. doi:10.5506/APhysPolB.48.259.
- [24] W. Satuła, J. Dobaczewski, W. Nazarewicz, T. R. Werner, Isospin-breaking corrections to superallowed Fermi β decay in isospin- and angular-momentum-projected nuclear density functional theory, *Phys. Rev. C* 86 (2012) 054316. doi:10.1103/PhysRevC.86.054316. URL <https://link.aps.org/doi/10.1103/PhysRevC.86.054316>
- [25] M. Wang, G. Audi, A. H. Wapstra, F. G. Kondev, M. MacCormick, X. Xu, B. Pfeiffer, The AME2012 atomic mass evaluation (II). Tables, graphs and references, *Chin. Phys. C* 36 (12) (2012) 1603–2014. URL <http://amdc.in2p3.fr/masstabes/Ame2012/Ame2012b-v2.pdf>
- [26] Evaluated Nuclear Structure Data File, <http://www.nndc.bnl.gov/ensdf/>.
- [27] K. Sato, J. Dobaczewski, T. Nakatsukasa, W. Satuła, Energy-density-functional calculations including proton-neutron mixing, *Phys. Rev. C* 88 (2013) 061301. doi:10.1103/PhysRevC.88.061301. URL <https://link.aps.org/doi/10.1103/PhysRevC.88.061301>
- [28] J. A. Sheikh, N. Hinohara, J. Dobaczewski, T. Nakatsukasa, W. Nazarewicz, K. Sato, Isospin-invariant Skyrme energy-density-functional approach with axial symmetry, *Phys. Rev. C* 89 (2014) 054317. doi:10.1103/PhysRevC.89.054317. URL <http://link.aps.org/doi/10.1103/PhysRevC.89.054317>
- [29] P. Bączyk, J. Dobaczewski, M. Konieczka, W. Satuła, Strong-interaction isospin-symmetry breaking within the density functional theory, *Acta Phys. Pol. B Proc. Supp.* 8 (3) (2016) 539–544. doi:<http://dx.doi.org/10.5506/APhysPolBSupp.8.539>.

- [30] W. Satuła, R. Wyss, Rotations in isospace: A doorway to the understanding of neutron-proton superfluidity in $N = Z$ nuclei, *Phys. Rev. Lett.* 86 (2001) 4488–4491. doi:10.1103/PhysRevLett.86.4488.
URL <http://link.aps.org/doi/10.1103/PhysRevLett.86.4488>
- [31] W. Satuła, R. Wyss, Microscopic structure of fundamental excitations in $N = Z$ nuclei, *Phys. Rev. Lett.* 87 (2001) 052504. doi:10.1103/PhysRevLett.87.052504.
URL <http://link.aps.org/doi/10.1103/PhysRevLett.87.052504>
- [32] W. Satuła, J. Dobaczewski, W. Nazarewicz, M. Rafalski, Isospin-symmetry restoration within the nuclear density functional theory: Formalism and applications, *Phys. Rev. C* 81 (2010) 054310. doi:10.1103/PhysRevC.81.054310.
URL <http://link.aps.org/doi/10.1103/PhysRevC.81.054310>
- [33] W. Satuła, J. Dobaczewski, M. Konieczka, W. Nazarewicz, Isospin mixing within the symmetry restored density functional theory and beyond, *Acta Phys. Pol. B* 45 (2014) 167. doi:10.5506/APhysPolB.45.167.
- [34] P. Bączyk, J. Dobaczewski, M. Konieczka, W. Satuła, T. Nakatsukasa, K. Sato, Strong-force isospin-symmetry breaking in masses of $N \sim Z$ nuclei, arXiv:1701.04628v2.
URL <https://arxiv.org/abs/1701.04628v2>
- [35] J. Toivanen, J. Dobaczewski, M. Kortelainen, K. Mizuyama, Error analysis of nuclear mass fits, *Phys. Rev. C* 78 (2008) 034306. doi:10.1103/PhysRevC.78.034306.
URL <https://link.aps.org/doi/10.1103/PhysRevC.78.034306>
- [36] J. Dobaczewski, W. Nazarewicz, P.-G. Reinhard, Error estimates of theoretical models: a guide, *Journal of Physics G: Nuclear and Particle Physics* 41 (7) (2014) 074001.
URL <http://stacks.iop.org/0954-3899/41/i=7/a=074001>
- [37] M. Wang, G. Audi, F. Kondev, W. Huang, S. Naimi, X. Xu, The ame2016 atomic mass evaluation (ii). tables, graphs and references, *Chinese Physics C* 41 (3) (2017) 030003.
URL <http://stacks.iop.org/1674-1137/41/i=3/a=030003>

- [38] D. Tarpanov, J. Toivanen, J. Dobaczewski, B. G. Carlsson, Polarization corrections to single-particle energies studied within the energy-density-functional and quasiparticle random-phase approximation approaches, *Phys. Rev. C* 89 (2014) 014307. doi:10.1103/PhysRevC.89.014307. URL <https://link.aps.org/doi/10.1103/PhysRevC.89.014307>
- [39] S. Shlomo, Nuclear Coulomb energies, *Reports on Progress in Physics* 41 (7) (1978) 957. URL <http://stacks.iop.org/0034-4885/41/i=7/a=001>
- [40] Y. Fujita, T. Adachi, H. Fujita, A. Algora, B. Blank, M. Csatlós, J. M. Deaven, E. Estevez-Aguado, E. Ganioglu, C. J. Guess, J. Gulyás, K. Hatanaka, K. Hirota, M. Honma, D. Ishikawa, A. Krasznahorkay, H. Matsubara, R. Meharchand, F. Molina, H. Okamura, H. J. Ong, T. Otsuka, G. Perdikakis, B. Rubio, C. Scholl, Y. Shimbara, E. J. Stephenson, G. Susoy, T. Suzuki, A. Tamii, J. H. Thies, R. G. T. Zegers, J. Zenihiro, High-resolution study of $T_z = +2 \rightarrow +1$ Gamow-Teller transitions in the $^{44}\text{Ca}(^3\text{He},t)^{44}\text{Sc}$ reaction, *Phys. Rev. C* 88 (2013) 014308. doi:10.1103/PhysRevC.88.014308. URL <http://link.aps.org/doi/10.1103/PhysRevC.88.014308>
- [41] M. MacCormick, G. Audi, Evaluated experimental isobaric analogue states from to and associated IMME coefficients, *Nuclear Physics A* 925 (2014) 61 – 95. doi:<http://dx.doi.org/10.1016/j.nuclphysa.2014.01.007>. URL <http://www.sciencedirect.com/science/article/pii/S0375947414000220>
- [42] X. Tu, Y. Litvinov, K. Blaum, B. Mei, B. Sun, Y. Sun, M. Wang, H. Xu, Y. Zhang, Indirect mass determination for the neutron-deficient nuclides ^{44}V , ^{48}Mn , ^{52}Co and ^{56}Cu , *Nuclear Physics A* 945 (2016) 89 – 94. doi:<http://dx.doi.org/10.1016/j.nuclphysa.2015.09.016>. URL <http://www.sciencedirect.com/science/article/pii/S0375947415002237>
- [43] X. Xu, P. Zhang, P. Shuai, R. J. Chen, X. L. Yan, Y. H. Zhang, M. Wang, Y. A. Litvinov, H. S. Xu, T. Bao, X. C. Chen, H. Chen, C. Y. Fu, S. Kubono, Y. H. Lam, D. W. Liu, R. S. Mao, X. W. Ma, M. Z. Sun, X. L. Tu, Y. M. Xing, J. C. Yang, Y. J. Yuan, Q. Zeng, X. Zhou, X. H. Zhou, W. L. Zhan, S. Litvinov, K. Blaum, G. Audi, T. Uesaka, Y. Yamaguchi, T. Yamaguchi, A. Ozawa, B. H. Sun, Y. Sun, A. C. Dai, F. R. Xu, Identification of the lowest $T = 2$, $J^\pi = 0^+$ isobaric analog state in ^{52}Co

- and its impact on the understanding of β -decay properties of ^{52}Ni , *Phys. Rev. Lett.* 117 (2016) 182503. doi:10.1103/PhysRevLett.117.182503.
URL <http://link.aps.org/doi/10.1103/PhysRevLett.117.182503>
- [44] D. A. Nesterenko, A. Kankainen, L. Canete, M. Block, D. Cox, T. Eronen, C. Fahlander, U. Forsberg, J. Gerl, P. Golubev, J. Hakala, A. Jokinen, V. S. Kolhinen, J. Koponen, N. Lalović, C. Lorenz, I. D. Moore, P. Papadakis, J. Reinikainen, S. Rinta-Antila, D. Rudolph, L. G. Sarmiento, A. Voss, J. Äystö, High-precision mass measurements for the isobaric multiplet mass equation at $A = 52$, *Journal of Physics G: Nuclear and Particle Physics* 44 (6) (2017) 065103.
URL <http://stacks.iop.org/0954-3899/44/i=6/a=065103>
- [45] G. A. Miller, B. M. K. Nefkens, I. Šlaus, Charge symmetry, quarks and mesons, *Physics Reports* 194 (1) (1990) 1 – 116.
doi:[http://dx.doi.org/10.1016/0370-1573\(90\)90102-8](http://dx.doi.org/10.1016/0370-1573(90)90102-8).
URL <http://www.sciencedirect.com/science/article/pii/0370157390901028>

Supplemental Material for: Isospin-symmetry breaking in masses of $N \simeq Z$ nuclei

P. Bączyk^a, J. Dobaczewski^{a,b,c,d}, M. Konieczka^a, W. Satuła^{a,d}, T.
Nakatsukasa^e, K. Sato^f

^a*Institute of Theoretical Physics, Faculty of Physics, University of Warsaw, ul. Pasteura
5, PL-02-093 Warsaw, Poland*

^b*Department of Physics, University of York, Heslington, York YO10 5DD, United
Kingdom*

^c*Department of Physics, P.O. Box 35 (YFL), University of Jyväskylä, FI-40014
Jyväskylä, Finland*

^d*Helsinki Institute of Physics, P.O. Box 64, FI-00014 University of Helsinki, Finland*

^e*Center for Computational Sciences, University of Tsukuba, Tsukuba 305-8577, Japan*

^f*Department of Physics, Osaka City University, Osaka 558-8585, Japan*

Abstract

Effects of the isospin-symmetry breaking (ISB) beyond mean-field Coulomb terms are systematically studied in nuclear masses near the $N = Z$ line. The Coulomb exchange contributions are calculated exactly. We use extended Skyrme energy density functionals (EDFs) with proton-neutron-mixed densities, to which we add new terms breaking the isospin symmetry. Two parameters associated with the new terms are determined by fitting mirror and triplet displacement energies (MDEs and TDEs) of isospin multiplets. The new EDFs reproduce MDEs for the $T = \frac{1}{2}$ doublets and $T = 1$ triplets, and TDEs for the $T = 1$ triplets. Relative strengths of the obtained isospin-symmetry-breaking terms *are not* consistent with the differences in the NN scattering lengths, a_{nn} , a_{pp} , and a_{np} . Based on low-energy experimental data, it seems thus impossible to delineate the strong-force ISB effects from beyond-mean-field Coulomb-energy corrections.

Keywords: nuclear density functional theory (DFT), energy density functional (EDF), proton-neutron mixing, isospin symmetry breaking (ISB), mirror displacement energy (MDE), triple displacement energy (TDE)

This Supplemental Material explains technical aspects of the method presented in the Letter and provides numerical results that complement those

of the Letter. We start by providing the reader with details concerning the choice of the basis size. Next, we discuss the subtleties related to the fitting procedure of the two new coupling constants. Finally, we present results obtained for the MDEs and TDEs calculated with the isospin-symmetry breaking (ISB) terms included in the SkM*^{ISB} [1] and SLy4^{ISB} [2] Skyrme functionals that mirror those for SV_T^{ISB} [3, 4], which were presented in the Letter.

1. Choice of the basis size

The code HFODD [5] used in this work solves the Hartree-Fock (HF) equations in the Cartesian harmonic oscillator (HO) basis. In this work, we use the spherical HO basis whose size is determined by the number of shells, N_0 , taken into account. Numerical stability with respect to N_0 was tested in detail in Ref. [6]. It turned out that the optimum choice of number of HO shells (in terms of the trade-off between precision and computing time) is $N_0 = 10$ for light nuclei ($10 \leq A \leq 30$), $N_0 = 12$ for medium-mass nuclei ($31 \leq A \leq 56$) and $N_0 = 14$ for heavier nuclei ($A \geq 57$). In the Letter, we followed these guidelines with exception of the $A = 58$ triplet, which was calculated with $N_0 = 12$ to maintain consistency with other triplets.

2. Adjustment of the model coupling constants

Results of fit of the model coupling constants t_0^{II} and t_0^{III} , together with essential elements of the fitting procedure, are given in the Letter. In the following subsections we provide further details concerning the methodology used. In particular, we discuss arguments justifying the splitting of the two-dimensional (2D) fit into two one-dimensional (1D) fits. We also discuss and quantify sources of potential errors and uncertainties.

2.1. Selecting HF solutions used for fitting

Calculations of MDEs and TDEs involve ground-state energies in even-even, odd- A , and odd-odd nuclei. In the even-even $A = 4n + 2$ triplets, the HF solutions representing the 0^+ ground states are unambiguously defined by filling the Kramers-degenerated levels from the bottom of the potential well up to the Fermi energy. However, in the odd- A $T = \frac{1}{2}$ doublets and $A = 4n$ $T = 1$ triplets, the HF solutions representing ground states are not uniquely defined. The ambiguity is related to the orientation of a current

generated by unpaired nucleon(s) with respect to the nuclear shape, which gives rise, in triaxial nuclei, to three different solutions that have angular momenta oriented along the intermediate (X), short (Y), and long (Z) axes of the nuclear shape [7]. No tilted-axis solutions were found. In $A = 4n$ $|T = 1, T_z = \pm 1\rangle$ states, one should consider, additionally, the aligned $|\nu \otimes \pi\rangle$ (or $|\bar{\nu} \otimes \bar{\pi}\rangle$) and anti-aligned $|\nu \otimes \bar{\pi}\rangle$ (or $|\bar{\nu} \otimes \pi\rangle$) arrangements of the valence neutron (ν) and proton (π). Let us mention that both the orientation and alignment ambiguities are related to the time-odd parts of the functional, which are very poorly constrained.

To test dependence of MDEs or TDEs on the orientation and alignment of the HF solutions, for SV_T^{ISB} we performed the complete set of calculations. We found that theoretical MDEs in both $T = \frac{1}{2}$ and $T = 1$ multiplets weakly depend on both the orientation and alignment. The corresponding uncertainty turned out to be of the order of 10 keV, and thus in the total uncertainty budget of MDE, it could be neglected. Accordingly, we performed calculations of MDEs using only the lowest-energy HF solutions obtained for any given Skyrme functional.

At variance with the results obtained for MDEs, for TDEs the influence of the orientations of the HF solutions turned out to be significant. Hence, in this case we computed TDEs for each of the three orientations separately, and then we averaged out the obtained results. The corresponding standard deviations associated with the averaging procedure was carried over to the total uncertainty budget. For SV_T^{ISB} , the fitting procedure was performed for ground-state configurations regardless of their alignment. This led to anti-aligned configurations in $A = 12, 20, 24, 36, 40, 44, 48,$ and 56 , and to aligned ones in the remaining $A = 4n$ triplets. In the $A = 4n$ triplets, the obtained values of K quantum numbers (projections of the angular momentum on the symmetry axis) agree with the experimental values of angular momentum I . The only exception is the $A = 12$ triplet, where we obtained $K = 2$ for $I = 1$. Furthermore, the procedure was tested for aligned and anti-aligned configurations separately. These two sets of solutions led to similar values of t_0^{II} coupling constant, and to similar predictions for the TDEs. Based on this observation, we decided to perform the calculations for other parametrizations with aligned solutions only, which are much easier to converge at the HF level.

Unfortunately, for certain values of A , we were unable to find solutions for all orientations. The missing solutions were: for SV_T^{ISB} , $A = 12$ and 16 ; for $\text{SkM}^{*\text{ISB}}$, $A = 12, 16, 20, 24, 28, 32, 40, 44,$ and 52 ; for SLy4^{ISB} , $A = 12,$

16, 28, 32, 40, and 52. Furthermore, for SkM*^{ISB} and SLy4^{ISB}, solutions for $A = 30$ and 36 triplets turned out to be spherically symmetric, which led to unexpectedly large values of TDE. Therefore, those points were excluded from fitting.

2.2. The fitting strategy

Our model has two free coupling constants, t_0^{II} and t_0^{III} (see Eqs. (3)–(6) of the Letter), which are adjusted to reproduce all available data on MDEs and TDEs in isospin doublets and triplets. The most general strategy would be to perform the 2D fit to the data, that is, to fit both coupling constants simultaneously. However, the 2D procedure is very costly computationally, as it requires both the doublets and triplets to be calculated in the pn -mixing formalism. Fortunately, coupling constants t_0^{II} and t_0^{III} are to a large extent independent of one another. Indeed, test calculations without Coulomb, performed in Ref. [8], clearly indicate that coupling constant t_0^{II} does not affect MDEs. The same calculations showed that the influence of coupling constant t_0^{III} on TDEs is also very weak, and comes mostly from a subtle modification of the HF solution due to the self-consistency of solutions. This property allows us to replace the rigorous 2D procedure by two constitutive 1D fits.

To reduce a possible discrepancy between the full 2D fit and our simplified fitting procedure, we first performed the adjustment of t_0^{III} coupling constant to MDEs. In the next step, for the physical value of t_0^{III} obtained previously, we performed the adjustment of t_0^{II} to TDEs. The adopted strategy allowed us to compute the doublets within the standard pn -separable formalism, thus reducing the computational effort considerably. Moreover, the calculations showed almost perfect linearity of MDEs (TDEs) as functions of t_0^{III} (t_0^{II}). For typical calculations, this fact is illustrated in Figs. 5 and 6. Such linearity, in turn, allowed us to compute derivatives of MDEs and TDEs over the coupling constants by using only two values of the coupling constants. Actually, to verify the linearity and to double-check the obtained results, we used three or four values. The errors introduced by the assumed linearity turned out to be negligible.

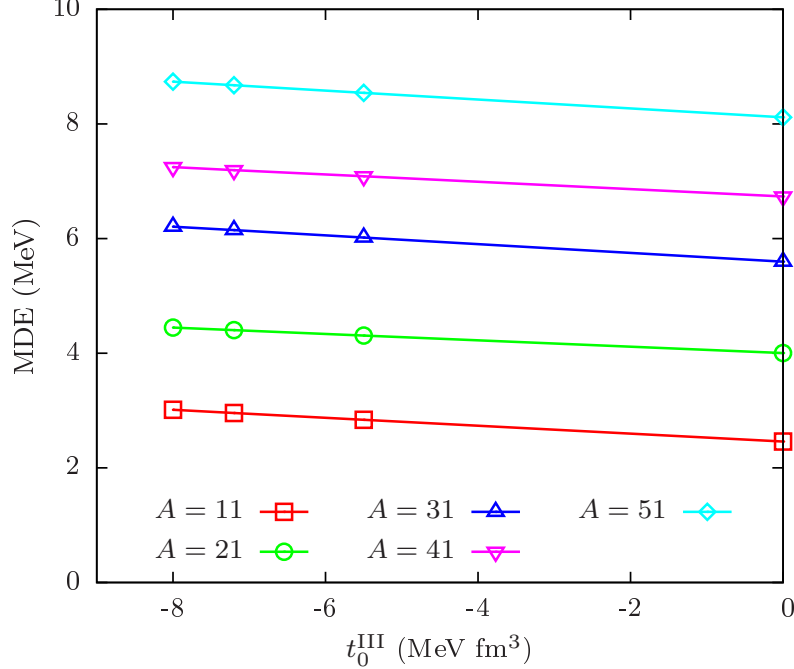


Figure 5: (Color online) MDEs of $T = \frac{1}{2}$ doublets calculated for different values of t_0^{III} ($t_0^{\text{II}} = 0$) and for SV_T^{ISB} . Calculated points are connected with line segments that are almost perfectly parallel to one another.

2.3. Penalty function and minimization procedure

The 1D fitting was based on the χ^2 minimization procedure described in Ref. [9]. We defined the penalty function χ^2 in the following way:

$$\chi^2(t_0) = \sum_{i=1}^{N_d} \frac{(\text{DE}_i(t_0) - \text{DE}_i^{\text{exp}})^2}{\Delta \text{DE}_i^2}, \quad (8)$$

where t_0 represents the actual coupling constants, t_0^{II} or t_0^{III} , used in the 1D fitting, N_d is the number of experimental data points, $\text{DE}_i(t_0)$ represents the displacement energies, MDEs or TDEs, calculated for a given value of coupling constant t_0 , and DE_i^{exp} are the experimental values of the displacement energies. The denominator, $\Delta \text{DE}_i^2 = (\Delta \text{DE}_i^{\text{exp}})^2 + (\Delta \text{DE}_i^{\text{the}})^2 + \Delta \text{DE}_{\text{mod}}^2$, is the error comprising three components:

- $\Delta \text{DE}_i^{\text{exp}}$ is the experimental error evaluated from errors of the binding and excitation energies as given in Refs. [10, 11],

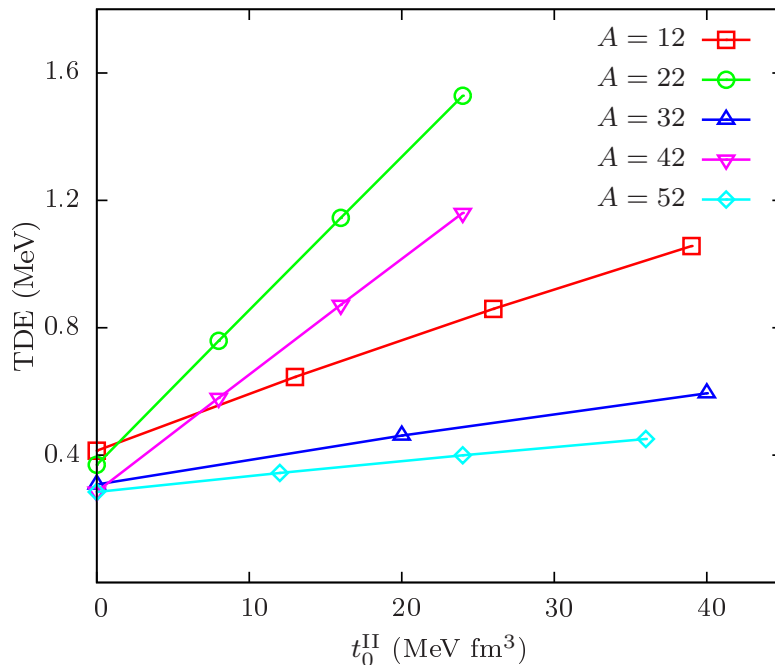


Figure 6: (Color online) TDEs of $T = 1$ triplets calculated for different values of t_0^{II} ($t_0^{\text{III}} = -7.4 \text{ MeV fm}^3$) and for SV_T^{ISB} . Calculated points are connected with line segments.

- $\Delta \text{DE}_i^{\text{the}}$ is the theoretical uncertainty related to the averaging over orientations as described above,
- $\Delta \text{DE}_{\text{mod}}$ is the theoretical model uncertainty, which is an unknown adjustable parameter.

The idea of the fit is to minimize χ^2 with the additional constraint of χ^2 per degree of freedom being equal to one. The latter condition can be obtained by adjusting the model uncertainty $\Delta \text{DE}_{\text{mod}}$, which is responsible for the spread of the theory-experiment differences. Values of model uncertainties obtained for three different Skyrme forces used in this work are collected in Table 3. As it turns out, the model uncertainty is the main source of the total uncertainty, which can be checked by comparing it with the root-mean-square deviations (RMSD) between theory and experiment, see Table 3.

Table 3: Values of the model uncertainties, ΔE_{mod} , and RMSD of MDEs and TDEs obtained for three EDFs considered in this work. All values are in keV.

	SV_T^{ISB}	$\text{SkM}^{*\text{ISB}}$	SLy4^{ISB}
$\Delta \text{MDE}_{\text{mod}}$	190	150	120
$\text{RMSD}(\text{MDE})$	200	150	120
$\Delta \text{TDE}_{\text{mod}}$	63	100	110
$\text{RMSD}(\text{TDE})$	69	100	110

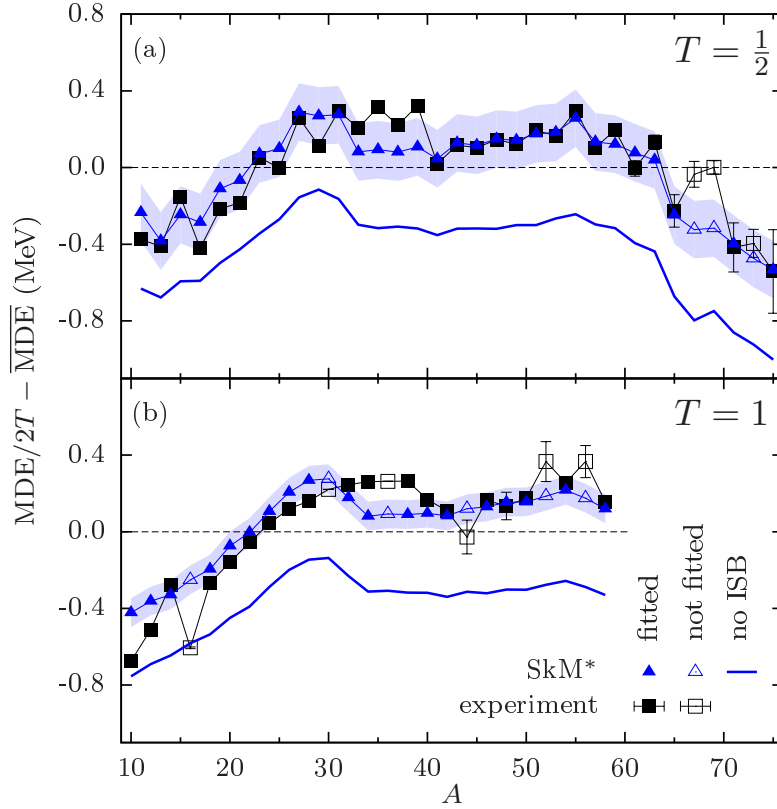


Figure 7: (Color online) Theoretical and experimental values of MDEs for the $T = 1/2$ (a) and $T = 1$ (b) mirror nuclei, shown with respect to the average linear trend defined in Fig. 1 of the paper. Calculations were performed using $\text{SkM}^{*\text{ISB}}$ functional with the ISB terms added. Shaded bands show theoretical uncertainties. Experimental error bars are shown only when they are larger than the corresponding symbols. Full (open) symbols denote data points included in (excluded from) the fitting procedure.

3. Complementary results for SkM*^{ISB} and SLy4^{ISB}

As stated in the Letter, calculations of MDEs and TDEs with the extended Skyrme forces involving the class-II and III contact terms were performed for three different Skyrme EDFs SV_T^{ISB} , SkM*^{ISB}, and SLy4^{ISB}. As shown in the Letter, within the model uncertainties, the resulting coupling constants t_0^{II} and t_0^{III} are fairly independent of the EDF. Below in Figs. 7–10, for the sake of completeness, we present results obtained for the EDFs SkM*^{ISB} and SLy4^{ISB}, whereas the analogous SV_T^{ISB} results were shown in Figs. 2 and 3 of the Letter. As we can see, for all three parametrizations, the agreement between experimental and theoretical values is similar. This nicely confirms that the method proposed in this work is indeed almost perfectly independent on the isoscalar charge-independent part of the functional. In this sense it is a quite robust method to assess the ISB effects in $N \simeq Z$ nuclei.

This work was supported in part by the Polish National Science Center under Contract Nos. 2014/15/N/ST2/03454 and 2015/17/N/ST2/04025, by the Academy of Finland and University of Jyväskylä within the FIDIPRO program, by Interdisciplinary Computational Science Program in CCS, University of Tsukuba, and by ImPACT Program of Council for Science, Tech-

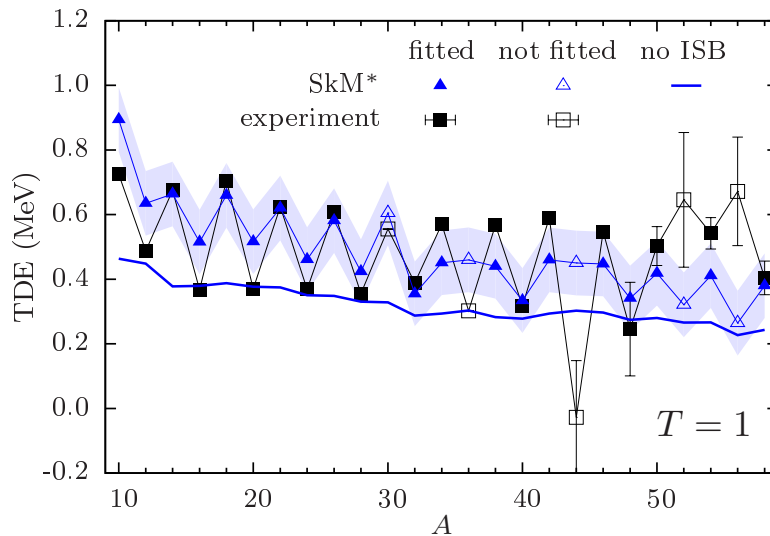


Figure 8: (Color online) Same as in Fig. 7 but for the $T = 1$ TDEs with no linear trend subtracted.

nology and Innovation (Cabinet Office, Government of Japan). We acknowledge the CIŚ Świerk Computing Center, Poland, and the CSC-IT Center for Science Ltd., Finland, for the allocation of computational resources.

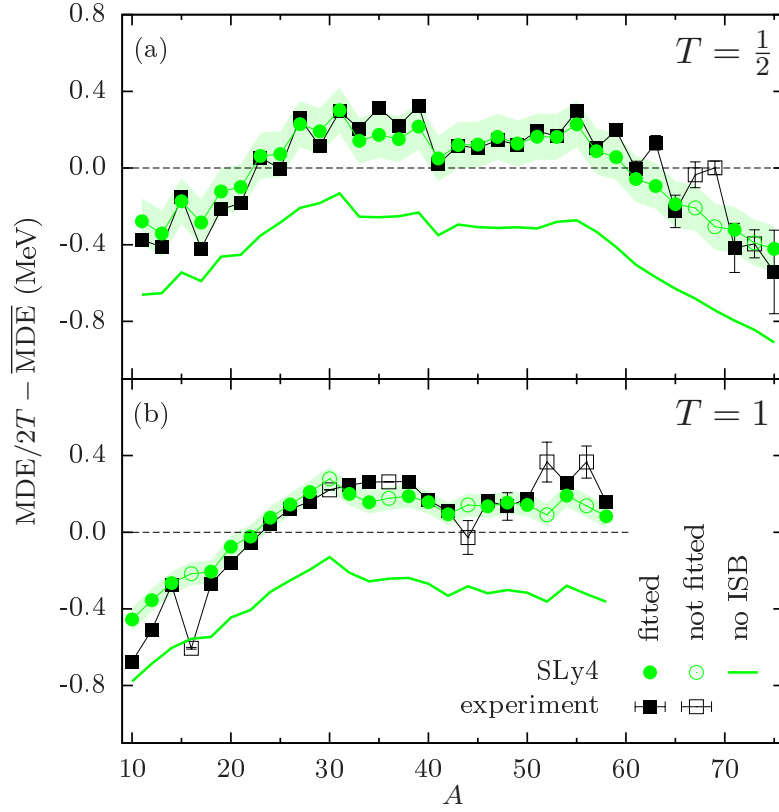


Figure 9: (Color online) Same as in Fig. 7 but for the SLy4^{ISB} EDF

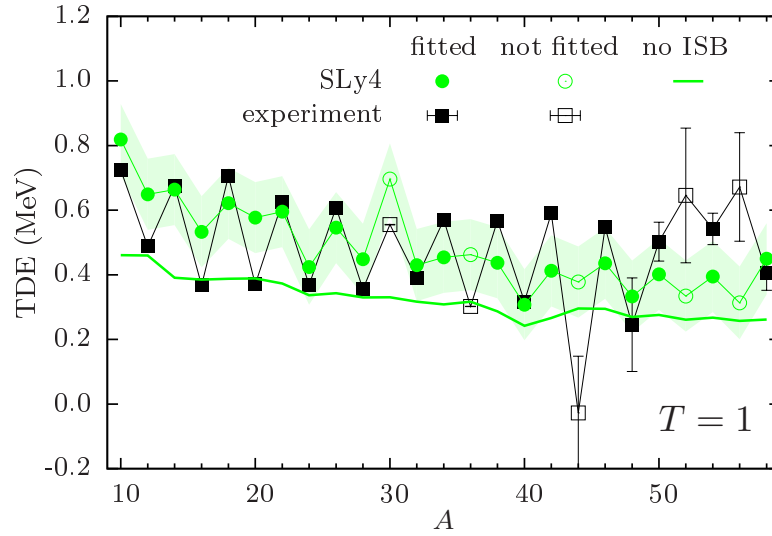


Figure 10: (Color online) Same as in Fig. 9 but for the $T = 1$ TDEs with no linear trend subtracted.

References

- [1] J. Bartel, P. Quentin, M. Brack, C. Guet, H.-B. Hkansson, Towards a better parametrisation of Skyrme-like effective forces: A critical study of the SkM force, *Nuclear Physics A* 386 (1) (1982) 79 – 100. doi:[https://doi.org/10.1016/0375-9474\(82\)90403-1](https://doi.org/10.1016/0375-9474(82)90403-1). URL <http://www.sciencedirect.com/science/article/pii/0375947482904031>
- [2] E. Chabanat, P. Bonche, P. Haensel, J. Meyer, R. Schaeffer, A Skyrme parametrization from subnuclear to neutron star densities Part II. Nuclei far from stabilities, *Nuclear Physics A* 635 (1) (1998) 231 – 256. doi:[https://doi.org/10.1016/S0375-9474\(98\)00180-8](https://doi.org/10.1016/S0375-9474(98)00180-8). URL <http://www.sciencedirect.com/science/article/pii/S0375947498001808>
- [3] M. Beiner, H. Flocard, N. V. Giai, P. Quentin, Nuclear ground-state properties and self-consistent calculations with the Skyrme interaction: (i). spherical description, *Nuclear Physics A* 238 (1) (1975) 29 – 69. doi:[https://doi.org/10.1016/0375-9474\(75\)90338-3](https://doi.org/10.1016/0375-9474(75)90338-3). URL <http://www.sciencedirect.com/science/article/pii/0375947475903383>

- [4] W. Satuła, J. Dobaczewski, Simple regularization scheme for multireference density functional theories, *Phys. Rev. C* 90 (2014) 054303. doi:10.1103/PhysRevC.90.054303. URL <https://link.aps.org/doi/10.1103/PhysRevC.90.054303>
- [5] N. Schunck, J. Dobaczewski, W. Satuła, P. Bączyk, J. Dudek, Y. Gao, M. Konieczka, K. Sato, Y. Shi, X. Wang, T. Werner, Solution of the Skyrme-Hartree-Fock-Bogolyubov equations in the Cartesian deformed harmonic-oscillator basis. (VIII) HFODD (v2.73y): A new version of the program, *Computer Physics Communications* 216 (2017) 145 – 174. doi:<https://doi.org/10.1016/j.cpc.2017.03.007>. URL <http://www.sciencedirect.com/science/article/pii/S0010465517300942>
- [6] P. Bączyk, J. Dobaczewski, M. Konieczka, T. Nakatsukasa, K. Sato, W. Satuła, Mirror and triplet displacement energies within nuclear DFT: Numerical stability, *Acta Phys. Pol. B* 48 (2017) 259. doi:10.5506/APhysPolB.48.259.
- [7] W. Satuła, J. Dobaczewski, W. Nazarewicz, T. R. Werner, Isospin-breaking corrections to superallowed Fermi β decay in isospin- and angular-momentum-projected nuclear density functional theory, *Phys. Rev. C* 86 (2012) 054316. doi:10.1103/PhysRevC.86.054316. URL <https://link.aps.org/doi/10.1103/PhysRevC.86.054316>
- [8] P. Bączyk, J. Dobaczewski, M. Konieczka, W. Satuła, Strong-interaction isospin-symmetry breaking within the density functional theory, *Acta Phys. Pol. B Proc. Supp.* 8 (3) (2016) 539–544. doi:<http://dx.doi.org/10.5506/APhysPolBSupp.8.539>.
- [9] J. Dobaczewski, W. Nazarewicz, P.-G. Reinhard, Error Estimates of Theoretical Models: a Guide, *J. Phys. G: Nucl. Part. Phys.* 41 (2014) 074001.
- [10] M. Wang, G. Audi, A. H. Wapstra, F. G. Kondev, M. MacCormick, X. Xu, B. Pfeiffer, The AME2012 atomic mass evaluation (II). Tables, graphs and references, *Chin. Phys. C* 36 (12) (2012) 1603–2014. URL <http://amdc.in2p3.fr/masstable/Ame2012/Ame2012b-v2.pdf>
- [11] Evaluated Nuclear Structure Data File, <http://www.nndc.bnl.gov/ensdf/>.